

COMPREHENSIVE THEORETICAL STUDY OF PYRIDO (2,3-b)PYRAZINE-2,3-DIOL BY USING DENSITY FUNCTIONAL THEORY

V.N. MISHRA[#], D.V. SHUKLA^{**}, V.K. SINGH^{***}, R. UPADHYAY^{****}, P. SINGH^{*****}, A.K. PANDEY^{***}, A. DWIVEDI^{*****}

^{*}Department of Physics, S.R.M.G.P.C., Lucknow (UP), India, [#]e-mail: vnvictorious@gmail.com

^{**}Department of Physics, GLA University, Mathura (UP), India

^{***}Department of Physics, "K.S. Saket" PG College, Ayodhya (UP), India

^{****}Department of Physics, Government Naveen College, Hasoud, Janjgir Champa (CG), India

^{*****}Department of Physics "Rajendra" College, Chapara (Bihar), India

^{*****}Department of Physics, "Seth Vishambhar Nath" Engineering College, Barabanki (UP), India

Abstract. In the present communication we have done theoretical study on molecular structure vibrational analysis electronic study and biological activity of pyrido (2,3-b)pyrazine-2,3-diol. The geometry optimization of title molecule was done by using combination of density functional theory (DFT) /B3LYP and 6-311G(d,p) basis set. The calculated spectra were interpreted with the help of normal mode analysis subsequent optimized structure of title molecule. The correlation factor $R^2 = 0.999$ shows that experimental frequencies are well matched with calculated frequencies. Electronic property of title molecule is calculated with help of Highest occupied molecular orbital (HOMO), Lowest unoccupied molecular orbital (LUMO), Molecular electronic surface plot (MESP). The docking of title molecule with 1FP1 protein suggests that title molecule have good medicinal potential.

Key words: Density functional theory, HOMO, LUMO, molecular docking, 1FP1 (protein).

INTRODUCTION

Pyrazine chemistry has been studied in 1974 by Belgand *et al.* [3], Dow Chemical's [5], and Nakamura *et al.* [19], due to its biological activity. At that time few derivatives were considered as dye chromophores, but production of pyrazinophthalocyanines was reported in 1990 [14]. Pyrido (2,3-b)pyrazine-2,3-diol and its derivative use as IP receptor which is during its activation have tremendous useful for the treatment of many pulmonary fibrosis as well as exert again good effects in fibrotic conditions of various organs in animal as well as

Received: March 2021;
in final form June 2021.

human models[4]. Its derivative may also use to degrade nicotine by the aerobic bacterium *Arthrobacter nicotinovorans*. Some of cases it may have intermediate role in investigating oxidation method in dying hair. A complete quantum chemical study may lead to assess every energetic as well as significant mechanistic insight within its formulation periphery.

In ongoing research [1, 6, 7, 15, 16, 20] we deal with the investigation of the structural, electronic, and vibrational properties of pyrido (2,3-b)pyrazine-2,3-diol. The structure and harmonic wave numbers were determined and analyzed at the density functional theory level employing 6-311G(d,p) as the basis set. The optimized geometry and its molecular properties, such as equilibrium energy, frontier orbital energy gap, molecular electrostatic potential (MESP) energy map, electronic and thermodynamic parameters of pyrido (2,3-b)pyrazine-2,3-diol were calculated and discussed. First principle calculations gives easier vibrational analysis of various spectroscopic modes of vibrations along with their intensity distribution.

MATERIALS AND METHODS

This computational scheme is very useful and extensively employed in the bio molecular studies due to reliability of its results as compared to experimental data. B3LYP functional [2, 13] are implemented, and all parameters are calculated with the efficient and accurate computational program Gaussian09 [9], by employing 6-311g(d,p) basis set. The HOMO, LUMO and MESP are plotted with help of GaussView program [8].

RESULTS

MOLECULAR STRUCTURE

The optimized structures of title molecule are calculated by using combination of DFT/B3LYP method and 6-311G(d,p) as the basis set and is shown in Fig. 1 with labeled atoms. The animated Gauss view shows that title molecule is unsymmetrical and contained two benzene rings fused to each other. The calculated C5-C6 bond length is 1.43 Å, the optimized N2-C5 bond length 1.37 Å is less than the standard bond length 1.47 Å. The optimized bond length of C8-H14 is 1.08 Å, which is in excellent agreement with the standard bond length of 1.09 Å. The other calculated bond lengths also show an excellent agreement with standard value. Based on the above comparison, it is clear that the calculated bond lengths are very near to the standard values.

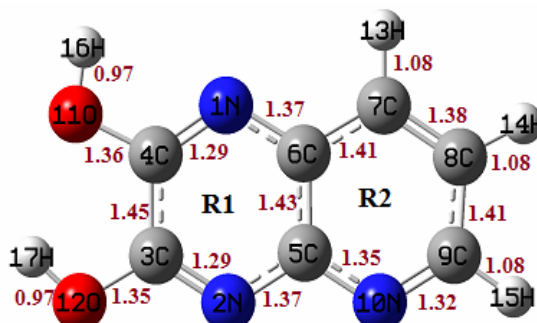


Fig. 1. Molecular structure of pyrido (2,3-b)pyrazine-2,3-diol by B3LYP 6-311G(d,p) level.

VIBRATIONAL SPECTROSCOPIC ANALYSIS

The pyrido (2,3-b)pyrazine-2,3-diol has 17 atoms and $3N-6(45)$ normal modes of fundamental vibration. The calculated frequencies are overestimate due to anharmonicity; electron-electron correlation so calculated wavenumbers are scaled by a factor of 0.96 [32] to compare with experimental wavenumber [24]. Detailed description of vibrational modes (Table 1) can be given by importance of normal coordinate analysis.

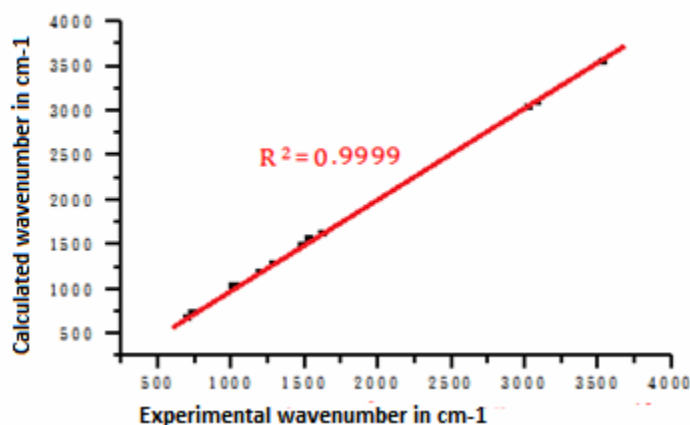


Fig. 2. Correlation between experimental wavenumbers and calculated wavenumbers.

Title molecule has $-\text{CH}$ and $-\text{OH}$ groups so, in higher wavenumber region, stretching vibrations [$\text{V}(\text{C-H})$ & $\text{V}(\text{O-H})$] are present. In this study, a sharp polarized peak appears at 3540 cm^{-1} ; it is well matched with calculated wavenumber 3541 cm^{-1} . This peak appears due to $\text{V}(\text{O-H})$. C-H bands fits well in the range $2800\text{--}3200 \text{ cm}^{-1}$. In the present study, two peaks appear at 3086 cm^{-1} and

3031 cm^{-1} , which are well matched with experimental wavenumber 3090 cm^{-1} and 3025 cm^{-1} , respectively, due to V(C-H). In lower wavenumber region two back-to-back peaks appears at 1618 cm^{-1} and 1555 cm^{-1} , due to $\beta(\text{CCN})\text{R1,R2}+\beta(\text{OH})\text{adjR1}$ and $\beta(\text{CC})\text{R1\&R2}$, respectively, which are well matched with experimental data. As we see that torsional modes are seen in the lower region. A strong torsion mode of H-C-C-H and N-C-C-N are at 590 cm^{-1} and 680 cm^{-1} in calculated spectrum. A correlation graph (Fig. 2) plotted in between experimental IR and calculated IR frequencies and find a linear correlation $Y = 6.62333 + 1.00327X$ with a correlation factor $R^2 = 0.999$. This correlation factor shows that experimental frequencies (FTIR, Fig. 3) are well matched with calculated IR frequencies.

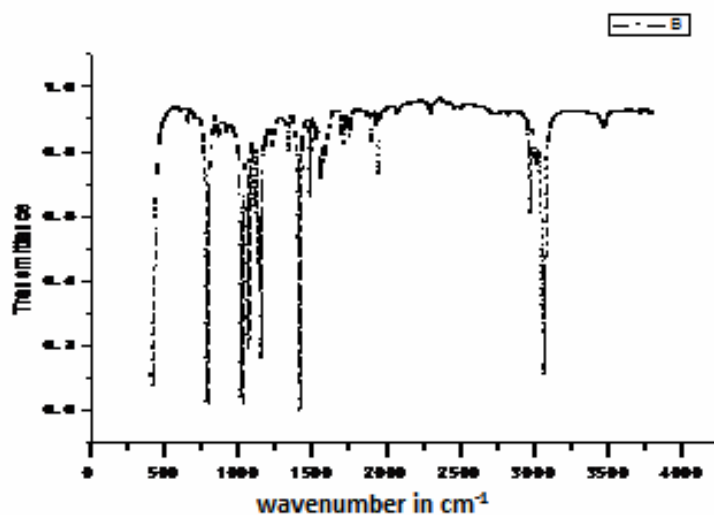


Fig. 3. The pyrido (2,3-b)pyrazine-2,3-diol infrared spectrum.

Table 1

Vibrational analysis at B3LYP/6-311G(d,p) level for pyrido (2,3-b)pyrazine-2,3-diol

Experimental wavenumber (cm^{-1})	Calculated wavenumber (cm^{-1})	IR intensity ($\text{K}\cdot\text{mmol}^{-1}$)	Mode of vibration
–	3655	143.40	V(H17-O12)adjR1
3540	3541	104.87	V(H16-O11)adjR1
3090	3086	13.12	[V(H13-C7)+V(H14-C8)]R2
–	3071	5.48	[V(H13-C7)+V(H14-C8)]R2
3025	3031	23.61	V(H15-C9)R2
1620	1618	14.19	$\beta(\text{CCN})\text{R1,R2}+\beta(\text{OH})\text{adjR1}$
–	1570	21.24	$\beta(\text{CCN})\text{R1,R2}+\beta(\text{OH})\text{adjR1}$
1535	1555	27.57	$\beta(\text{CC})\text{R1\&R2}$

1490	1494	8.54	$\beta(\text{CC})\text{R1,R2}+\text{S}(\text{CCH})\text{R2}$
–	1456	118.25	$\beta(\text{CC})\text{R1,R2}+\text{S}(\text{CCH})\text{R2}$
–	1437	517.31	$\text{S}(\text{H14-C8-C9-H15})\text{R2}$
–	1348	11.22	$\beta(\text{CCC})\text{R2}$
–	1339	87.28	$\omega(\text{H13-C7-C8-H14})\text{R2}$
–	1302	306.31	$\beta(\text{CCC})\text{R2}+\text{S}(\text{H15-O11-C4})\text{adjR1}$
1290	1288	24.72	$\beta(\text{CCC})\text{R1}\&\text{R2}$
–	1219	3.79	$\beta(\text{HCCH})\text{R2}+\text{S}(\text{HOC})\text{adjR1}$
1200	1194	21.54	$\beta(\text{CCC})\text{R2}+\text{t}(\text{H15-C9-N10})\text{R2}$
–	1178	23.74	$\beta(\text{CC})\text{R1}\&\text{R2}+\text{t}(\text{H17-O12-C3})\text{R1}$
–	1139	305.77	$\text{S}(\text{H16-O11-C4})\text{adjR1}$
–	1093	13.16	$\text{S}(\text{H13-C7-C8-H14})\text{R2}$
1020	1024	1.03	$\text{S}(\text{H14-C8-C9-H15})\text{R2}$
–	911	5.75	$\text{t}(\text{C7-C8-C9-N10})\text{R2}+\omega(\text{HOC})\text{adjR1}$
–	869	11.04	$\beta(\text{CCC})\text{R1}\&\text{R2}$
740	729	7.48	$\beta(\text{CCC})\text{R1}$
–	711	3.85	Breathing $\text{R1}\&\text{R2}+\omega(\text{HCCH})\text{R2}$
700	680	3.72	$\text{t}(\text{H14-C8-C9-H15})\text{R2}$
–	606	35.80	Breathing $\text{R1}\&\text{R2}+\text{t}(\text{H13-C7-C8-H14})\text{R2}$
–	590	11.68	$\text{t}(\text{HCCH})\text{R2}+\text{t}(\text{NCCN})\text{R1}$
–	519	63.88	Breathing R2
480	463	0.76	$\text{R}(\text{H14-C8-C9-H15})\text{R2}$
–	457	7.97	$\omega(\text{HCCH})\text{R1}+\beta(\text{CCC})\text{R1}\&\text{R2}$
–	451	129.19	$\omega(\text{H17-O12-C3})\text{R1}$
–	412	47.36	Breathing $\text{R1}\&\text{R2}+\omega(\text{HOC})\text{R1}$
–	348	0.27	$\omega(\text{H16-O11-C4})\text{R1}+\text{t}(\text{HCCH})\text{R1}\&\text{R2}$
–	309	5.48	Breathing $\text{R1}\&\text{R2}+\omega(\text{HCCH})\text{R2}$
–	307	4.29	$\beta(\text{HCCH})\text{R1}+\beta(\text{H17-O12-H15})\text{R1}$
–	265	0.04	$\omega(\text{H16-O11-C4})\text{R1}+\text{t}(\text{HCCH})\text{R1}\&\text{R2}$
–	133	3.52	Twisting $\text{R1}\&\text{R2}+\gamma(\text{HCCH})\text{R2}$

HOMO-LUMO AND MESP PLOTS AND ELECTRONIC PARAMETERS

The frontier molecular orbital's (HOMO-LUMO) and their properties such as energy are very useful for physicist and chemists. This is also useful for predicting the most reactive position in pie-electron system and explains several types of reaction in conjugated system [23]. The conjugated molecules are characterized by a small highest occupied molecular orbital and lowest unoccupied molecular orbital (HOMO-LUMO) separation, which is the result of significant degree of intra-molecular charge transfer from the end-capping electron-donor groups to the efficient electron acceptor groups through pie-conjugated path [21]. The HOMO,

LUMO and MESP plots of title molecule are shown in Fig. 4. Both HOMO and LUMO are distributed over whole molecule. The energy gap of pyrido (2,3-b)pyrazine-2,3-diol is 4.71 eV. In color grading scheme, the blue represents the most electropositive (O10, O11), i.e., electron poor region, whereas the red (N2) corresponds to the most electronegative center, i.e., electron rich region [17, 24].

Ionization energies, I , and electron affinity, A , are calculated as the negative of energy eigen values of HOMO and LUMO respectively. χ and η can be calculated by using finite-difference approximations [22] as $\eta = \frac{1}{2}(I - A)$ and $\chi = \frac{1}{2}(I + A)$. These parameters, often used to describe chemical reactivity of molecules, are listed in Table 2, where: $I.P.$ = ionization potential, $E.A.$ = electron affinity, χ = electronegativity, η = global hardness, S = global softness, ω = global electrophilicity index, E_g = band gap.

Table 2

Calculated electronic properties of pyrido (2,3-b)pyrazine-2,3-diol by B3LYP 6-311G(d,p) level

$I.P.$ (eV)	$E.A.$ (eV)	η (eV)	χ (eV)	S (eV)	ω (eV)	E_g (eV)
8.70	0.22	4.24	4.46	0.12	4.69	4.71

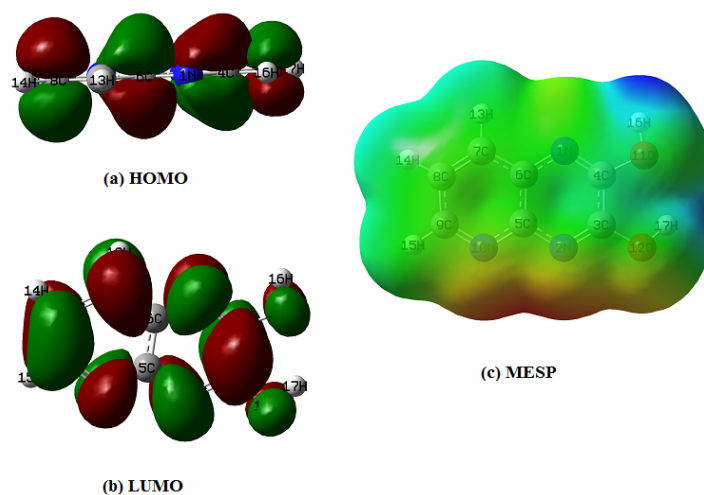


Fig. 4. HOMO, LUMO and MESP surfaces of pyrido (2,3-b)pyrazine-2,3-diol.

BIOLOGICAL ACTIVITIES AND DOCKING

ALOGPS 2.1 [25] program, developed by Tetko *et al.* [14, 26, 27], is based on electro topological indices like $\text{Log } P$ and $\text{Log } S$. The parameter $\text{Log } P$ is basically employed to determine transport properties of drug through cell membranes. In this

study the calculated the value of $\text{Log } P$ (0.31) recommends that the title molecule shows good ability to transport through cell membranes. The calculated value $\text{Log } S$ (-.35) lies in between -1 to -5.36 (more than 85 % drugs) favors the permeability of title compound into cell membranes. Several biological activities are calculated with help of PASS software of title molecule. The prediction of biological activities by PASS [28] based on the analysis of structure activity relationships (SAR). By using molecular mechanisms, PASS calculate 900 pharmacological properties, e.g., mutagenicity, carcinogenicity, teratogenicity, and embryo toxicity. The calculated biological activities of title molecule for $Pa > 70\%$ is listed in Table 4. Title molecule shows good activities against glycosylphosphatidylinositol phospholipase D inhibitor (0.845), dehydro-L-gulonate decarboxylase inhibitor (0.832), lysostaphin inhibitor (0.752), nicotinate dehydrogenase inhibitor (0.744), etc. These activities are related to pulmonary fibrosis so to design new pulmonary fibrosis drug we have performed docking of title molecule with appropriate protein. Swiss dock is online server is used to perform docking. Swiss dock [11, 33] predict isoliquiritigenin 2'-o-methyltransferase (1FP1) protein for docking. The 3D protein structure of 1FP1 is obtained at protein data bank [10]. The calculated full fitness score (-916.51 kcal/mol) and binding affinity (-.22 kcal/mol) shows that title molecule binds well with target protein [21, 29, 31]. The docking picture is obtained by CHIMERA 3.0 software and plotted in Fig. 5. From this figure, we see that nitrogen of title molecule bind with amphipathic amino acid methionine (MET17) residue with 2.27 Å distance.

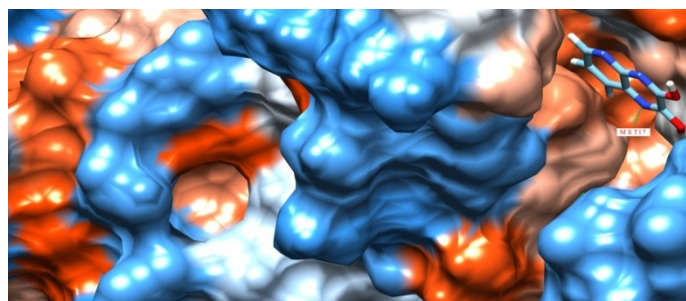


Fig. 5. Docking of title molecule with 1FP1 protein.

Table 3

Calculated biological activity of title molecule by PASS for $Pa > 70\%$

S.N.	Biological activity	Pa	Pi
1	Glycosylphosphatidylinositol phospholipase D inhibitor	0,845	0,006
2	Dehydro-L-gulonate decarboxylase inhibitor	0,832	0,006
3	Nicotinic alpha2beta2 receptor	0,780	0,013

	antagonist		
4	Nicotinate dehydrogenase inhibitor	0,744	0,004
5	Nicotinic alpha6beta3beta4alpha5 receptor antagonist	0,759	0,019
6	tRNA-pseudouridine synthase I inhibitor	0,731	0,005
7	NADPH peroxidase inhibitor	0,715	0,024
8	Aspulvinonedimethylallyltransferase inhibitor	0,703	0,063

P_a = pharmacologically active index, P_i = pharmacologically inactive index.

CONCLUSIONS

This study presents a complete computational structural study of pyrido (2,3-b)pyrazine-2,3-diol. All calculated wavenumbers are real in nature; thus, it is stable. All vibrational modes are thoroughly described first time by using first principle methods which act vital role for description of various chemical assignments. The calculated full fitness score and binding affinity shows that title molecule binds well with target protein.

Conflict of interest: The authors declare that they have no conflict of interest.

REFERENCES

1. BAJPAI, A., A.K. PANDEY, K. PANDEY, A. DWIVEDI, Reactive nature, substitution reaction, structural and vibrational properties of 2,3dichloropridine by DFT study, *Journal of Computational Methods in Molecular Design*, 2014, **4**(1), 64–69.
2. BECKE, A.D., Density functional thermochemistry-I. The effect of the exchange-only gradient correction, *J. Chem., Phys.*, 1993, **98**, 5648–5652.
3. BEGLAND, R.W., D.R. HARTTER, D.S. DONALD, A. CAIRNCROSS, W.A. SHEPPARD, Hydrogen cyanide chemistry. VII. Diiminosuccinonitrile condensation with diaminomaleonitrile, *The Journal of Organic Chemistry*, 1974, **39**(9), 1235–1239.
4. CHALTRON, S.J., C. LEBLANC, S.C. MCKEOWN, *USA Patent US*, 2015, **9**,132,127B2.
5. Dow Chemical Co., US Patent 3,879,394 (1975) and 4,199,581 (1978), *Chem. Abstract.*, **83**, 133, 397.
6. DWIVEDI, A., A.K. PANDEY, N. MISRA, Comparative study of vibrational spectra of two well-known natural products lupeol and lupenone using density functional theory, *Spectroscopy: An International Journal*, 2012, **27**, 155–166.
7. DWIVEDI, A., A.K. PANDEY, N. MISRA, Electronic structure, optical properties and vibrational analysis of 2-decenoic acid and its derivative by density functional theory, *Spectroscopy: An International Journal*, 2011, **26**, 367–385.
8. FRISCH, A., A.B. NELSON, A.J. HOLDER, *Gauss View* Pittsburgh, USA, 2005.
9. FRISCH, M.J., G.W. TRUCKS, H.B. SCHLEGEL, G.E. SCUSERIA, M.A. ROBB, J.R. CHEESEMAN, G. SCALMANI, V. BARONE, B. MENNUCCI, G.A. PETERSSON, H. NAKATSUJI, M. CARICATO, X. LI, H.P. HRATCHIAN, A.F. IZMAYLOY, J. BLOINO, G. ZHENG, J.L. SONNENBERG, M. HADA, M. EHARA, K. TOYOTA, R. FUKUDA, J.

- HASEGAWA, M. ISHIDA, T. NAKAJIMA, Y. HONDA, O. KITAO, H. NAKAI, T. VREVEN, J.A. MONTGOMERY, JR., J.E. PERALTA, F. OGLIARO, M. BEARPARK, J.J. HEYD, E. BROTHERS, K.N. KUDIN, V.N. STAROVEROV, R. KOBYASHI, J. NORMAND, K. RAGHAVACHARI, A. RENDELL, J.C. BURANT, S.S. IYENGER, J. TOMASI, M. COSSI, N. REGA, J.M. MILLAM, M. KLENE, J.E. KNOX, J.B. CROSS, V. BAKKEN, C. ADAMO, J. JARAMILLO, R. GOMPERS, R.E. STRATMANN, O. YAZYEV, A.J. AUSTIN, R. CAMMI, C. POMELLI, J.W. OCHTERSKI, R.L. MARTIN, K. MOROKUMA, V.G. ZAKRZEWSKI, G.A. VOTH, P. SALVADOR, J.J. DANNENBERG, S. DAPPRICH, A.D. DANIELS, O. FARKAS, J.B. FORESMAN, J.V. ORTIZ, J. CIOSLOWSKI, D.J. FOX, *Gaussian 09, Revision B.1, Gaussian*, Wallingford, UK, 2010.
10. GROSDIDIER, A., V. ZOETE, O. MICHIELIN, Fast docking using the CHARMM force field with EADock DSS, *J. Comput. Chem.*, 2011, **32**, 2149–2159.
 11. GROSDIDIER, A., V. ZOETE, O. MICHIELIN, SwissDock, a protein-small molecule docking web service based on EADock DSS, *Nucleic Acids Res.*, 2011, **39**, 270–277.
 12. KRISHNAN, R., J.S. BINKLEY, R. SEEGER, J.A. POPE, Self-consistent molecular orbital methods. XX. A basis set for correlated wave functions, *J. Chem. Phys.*, 1980, **72**, 650–654.
 13. LEE, C., W. YANG, R.G. PARR, Development of the Colle-Salvetti correlation-energy formula into a functional of the electron density, *Phys. Rev. B*, 1998, **133**(7), 785–789.
 14. LIZASA, Y.Y., MAGUCHI, M. TAGAWA, H. SAITO, T. FUJISAWA, K. KATO, M. TANIGUCHI, Establishment of human monoclonal antibody recognizing a new tumor-associated antigen from a patient with small cell lung carcinoma, *Hybridoma*, 1990, **9**, 211–219.
 15. LIVINGSTONE, J.J., D.J. TETKO, Neural network modeling for estimation of partition coefficient based on atom-type electrotopological state indices, *J. Chem. Inf. Comput. Sci.*, 2000, **40**(4), 947–455.
 16. MISRA, N., A. DWIVEDI, A.K. PANDEY, S. TRIVEDI, Vibrational analysis of two narcotic compounds – codeine and morphine – A comparative DFT study, *Der Pharma Chemica*, 2011, **3**(3), 427–448.
 17. MISRA, N., O. PRASAD, L. SINHA, A. PANDEY, Molecular structure and vibrational spectra of 2-formylbenzotrile by density functional theory and *ab initio* Hartree-Fock calculations, *Journal of Molecular Structure: THEOCHEM*, 2007, **822**, 45–47.
 18. MURRAY, J.S., K. SEN, *Molecular Electrostatic Potential, Concepts and Applications*, Elsevier, Amsterdam, The Netherlands, 1996.
 19. NAKAMURA, A., T. ATAKA, H. SEGAWA, Y. TAKEUCHI, T. TAKEMATSU, Structure-activity relationship in herbicidal activity of 5-chloro-2,3-dicyanopyrazines against barnyard grass, *Agric. Biol. Chem.*, 1983, **47**, 1555–1561.
 20. PANDEY, A.K., A. DWIVEDI, N. MISRA, Quantum Mechanical study on the structure and vibrational spectra of cyclobutanone and 1,2-cyclobutanedione, *Spectroscopy*, 2013, **30**, 210–221.
 21. PULAY, P., G. FOGARASI, G. PONGAR, J.E. BOGGS, A. VARGHA, Combination of theoretical *ab initio* and experimental information to obtain reliable harmonic force constants. Scaled quantum mechanical (QM) force fields for glyoxal, acrolein, butadiene, formaldehyde, and ethylene, *J. Am. Chem. Soc.*, 1983, **105**, 7037–7047.
 22. RAJA, M., R.R. MUHAMED, M.S. MUTHU, M. SURESH, Synthesis, spectroscopic (FT-IR, FT-Raman, NMR, UV-Visible), first order hyperpolarizability, NBO and molecular docking study of (E)-1-(4-bromobenzylidene)semicarbazide, *Journal of Molecular Structure*, 2017, **1128**, 481–492.
 23. ROZAS, I., I. ALKORTA, J. ELGUERO, Behavior of ylides containing N, O, and C atoms as hydrogen bond acceptors, *J. Am. Chem. Soc.*, 2000, **122**, 11154–11161.

24. SCOTT, A.P., L. RANDOM, Harmonic vibrational frequencies: An evaluation of Hartree-Fock, Møller-Plesset, quadratic configuration interaction, density functional theory, and semiempirical scale factors, *J. Phys. Chem.* 1996, **100**, 16502–16513.
25. SPONER, J., P. HOBZA, DNA base amino groups and their role in molecular interactions: *Ab initio* and preliminary density functional theory calculations, *International Journal of Quantum Chemistry*, 1996, **57**, 959–970.
26. TETKO, I.V., V.K. TANCHUK, Application of associative neural networks for prediction of lipophilicity in ALOGPS 2.1 program, *J. Chem. Inf. Comput. Sci.*, 2002, **42**, 1136–1145.
27. TETKO, I.V., V.Y. TANCHUK, T.A. KASHEVA, A.E. VILLA, Estimation of aqueous solubility of chemical compounds using E-state indices, *J. Chem. Inf. Comput. Sci.*, 2001, **41**, 1488–1493.
28. TETKO, I.V., V.Y. TANCHUK, T.A. KASHEVA, A.E. VILLA, Prediction of n-octanol/water partition coefficients from PHYSPROP database using artificial neural networks and E-state indices, *J. Chem. Inf. Comput. Sci.*, 2001, **41**, 1407–1421.
29. TETKO, I.V., V.Y. TANCHUK, T.N. KASHEVA, A.E. VILLA, Internet software for the calculation of the lipophilicity and aqueous solubility of chemical compounds, *J. Chem. Inf. Comput. Sci.*, 2001, **41**, 246–252.
30. TIWARI, G., A.K. SRIVASTAVA, R. KUMAR, A. KUMAR, Quantum chemical and molecular docking studies on two potential hepatitis C virus inhibitors, *Main Group Chemistry*, 2019, **18**, 107–121.
31. YADAV, K.K., A. KUMAR, S. BEGAM, K. NURJAMAL, G. BRAHMACHARI, N. MISRA, Spectroscopic (FTIR, UV-Vis and NMR), theoretical investigation and molecular docking of substituted 8-dioxodecahydroacridine derivatives, *J. Serb. Chem. Soc.*, 2019, **84**, 1–14.
32. ***<https://webbook.nist.gov/cgi/inchi?ID=C2067847&Mask=80#IR-Spec>.
33. ***<https://www.rcsb.org/structure/5AJG>.